EUROFUSION WPS1-CP(16) 15724

M. Nagel et al.

First evaluation of cryogenic performance of Wendelstein 7-X cryostat

Preprint of Paper to be submitted for publication in Proceedings of 29th Symposium on Fusion Technology (SOFT 2016)

This work has been carried out within the framework of the EUROfusion Consortium and has received funding from the Euratom research and training programme 2014-2018 under grant agreement No 633053. The views and opinions expressed herein do not necessarily reflect those of the European Commission.

First evaluation of cryogenic performance of Wendelstein 7-X cryostat

M. Nagel, C.P. Dhard, H. Bau, U. Meyer, S. Raatz, T. Rummel, K. Risse, H.-S. Bosch, and the W7-X Team

Max-Planck-Institut für Plasmaphysik, Greifswald, Germany

Commissioning [1] and the first operational phase of the stellarator Wendelstein 7-X (W7-X) have been accomplished successfully at the Greifswald branch of the Max-Planck-Institut für Plasma Physik. First helium plasma was achieved on 10th of December 2015 followed by the first hydrogen plasma in February 2016. The plasma is confined by a magnetic field of 2.5 T on the plasma axis created by a superconducting magnet system of 70 coils. The coils are located in a cryostat and protected against thermal radiation by vacuum and a thermal shield. Cooling of the coils and of the shield is provided with a helium refrigerator keeping the magnet system at 4 K and the shield at 70 K.

The paper presents the cooling concept of the thermal shield and of the coils with the coil structures. It describes the results of the first cool down of the cryostat to 4 K and the resulting heat loads at the different temperature levels. The experimental data show that the heat loads are well below the plant capacity allowing safe magnet operation.

Keywords: Cryogenics, superconducting magnet, Wendelstein 7-X, thermal shield

1. Introduction

The hot plasma of the stellarator fusion experiment W7-X is confined within a magnetic cage which is generated by a superconducting magnet system consisting of 50 Non Planar Coils (NPC) and 20 Planar Coils (PLC). High Temperature Superconducting Current Leads (CL) connect the cold superconducting bus bars with current feeders at ambient temperature outside the cryostat. The coils and their support structures are cooled with supercritical helium at 3.9 K. The cooling is provided by a helium-refrigerator with an equivalent cooling power of 7 kW at 4.5 K.

Magnet system and cold structures are located inside an evacuated cryostat. 254 ports equipped with supply and return lines and plasma diagnostics pass the insulation vacuum and connect the Outer Vessel (OV) with the inside of the Plasma Vessel (PV). A schematic cross section of the cryostat is shown in Fig. 1.

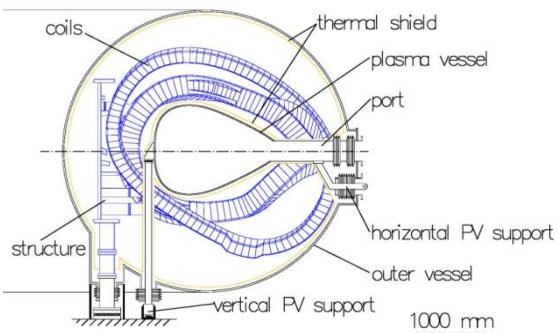

Fig.1. Cross section of W7-X cryostat showing the plasma vessel, the coils, the cold structure and the thermal shield.

The cryostat is divided in five modules based on the fivefold symmetry of the magnetic field. The symmetry of the cryostat components is partially realized leading to five similar but not identical modules, divided in two Half Modules (HM) and numbered X0 and X1 (X = 1-5).

2. Description of the Thermal insulation

2.1 Design Concept

The warm surfaces inside the cryostat are covered with Multi Layer Insulation (MLI) and an actively cooled thermal radiation shield. Redundant cooling pipes (Ø10x1.5 mm and Ø17x1.5 mm) are attached to the shields using copper braids. They are cooled by a forced flow of gaseous helium. The thermal shield sectors cover the OV, the PV and the port insulation. Within a HM the cooling pipes supply first the OV and then the PV panels. All 10 HM are cooled in parallel. The port shields don't have their own cooling pipes. They are conductively cooled through the OV and PV panels. More details on the basic design of the thermal insulation are given in [2].

2.2 Plasma vessel shield

The thermal shield of one module of the PV is divided into 40 panels. The panels are made of 4.5 mm thick glass fiber epoxy with embedded copper meshes. Each panel is connected to two parallel cooling pipes via copper braids. Fig. 2 shows a CAD-model the PV-shield with cooling pipes and holes for the ports. The positions of the attached temperature sensors are marked.

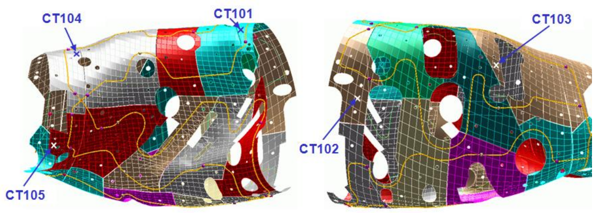

Fig. 2. PV-shield with cooling pipes (yellow) and the location of temperature sensors CT101, CT102, CT103, CT104, and CT105.

author's email:michael.nagel@ipp.mpg.de

2.3 Outer vessel shield

The modules of the OV are divided into an upper and a lower half shell. The thermal shields of a half shell are divided into panels made of rolled brass sheets with a thickness of 3 mm. The cooling loops from the upper and from the lower shell are connected in series. The pipes are connected to the panel with copper strips that are welded to the panels and soldered to the cooling pipes. Fig. 3 shows a CAD-model of the lower shell panels with cooling pipes and holes for the ports. The positions of the temperature sensors are also marked.

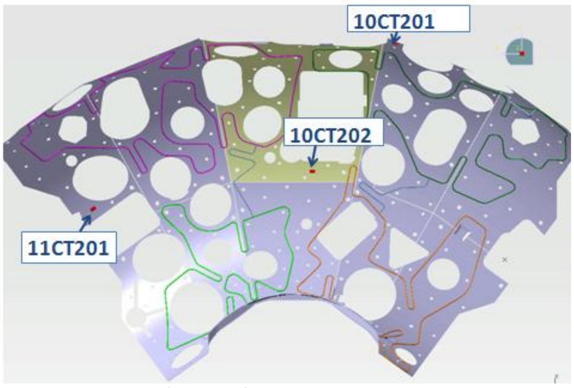

Fig. 3. Lower half shell of OV-shield with cooling pipes. The locations of temperature sensors are marked (11CTCT201, 10CTCT201, 10CTCT201).

2.3 Port insulation

Ports are circular, oval or rectangular tubes with diameters varying between 200 mm and 1000 mm. They run from the OV to the PV inside the cryostat. The port shields cover the ports and are divided in the inner and the outer tube (see Fig. 4); as the ports have no cooling pipes, the inner tube is thermally connected to the PV shield, the outer tube to the OV-shield.

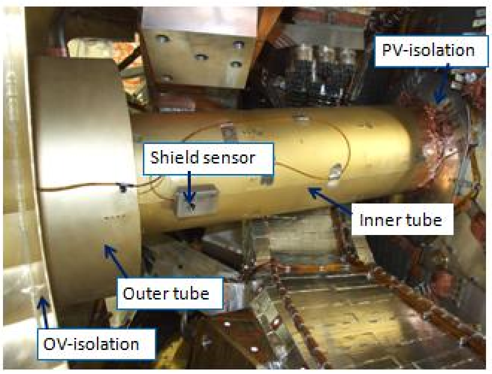

Fig. 4. Port thermal shield consisting of outer tube and, inner tube. In addition the temperature sensor is marked.

2.4 Location of temperature sensors

The thermal shield of a HM is equipped with 5 PT100 temperature sensors on the PV-shield panels, 1 sensor at the inner port shield and two sensors at the OV-panels. Additionally 3 TVO sensors are used to measure the He- temperatures of the shield cooling circuit, inlet and outlet of the OV- shield cooling named CT603, CT601, and the outlet temperature of the PV-shield cooling (CT604).

Three PV-shield sensors of a HM are located on the panel surface not far away from the cooling pipes and represent an ideal design configuration (CT101, CT102, CT105). Two sensors are located close to big port shields and see the thermal loads coming from the port shields (CT102, CT103).

The outer vessel panels are equipped with 4 sensors for a module, three in the lower half shell and one in the upper shell. Two sensors are located close to big ports but not far away from the cooling pipes (10CT201, 10CT202). The third sensor is far away from a cooling pipe and is close by big domes and port shields (11CT201). The same is true for the fourth sensor that is located in the upper shell (11CT202). The third and the fourth sensors give temperature information on hot spots only. The sensor positions are the same in the different modules. The port shields have one sensor close to the interface of the inner tube to outer tube (see Fig. 4).

3. Transient behavior of the cryostat

3.1 Cool down

After commissioning of the cryogenic system the cool down of the magnet system and the thermal shield were done in parallel with the cool down of the refrigerator in March 2015 (see [3]). A maximum cool down rate of 1 K/h was defined with a temperature difference between helium inlet and the maximum of the cooled components smaller than 40 K. The second criterion limited the cool down rate which was much slower than 1 K/h at the beginning. The mass flow distribution in the different cooling circuits was adjusted daily to ensure uniform cool down. Cool down started at a cryostat vacuum of about $2*10^{-4}$ mbar. The pressure dropped to 10^{-7} mbar with the cool down of the coils [4]. Vacuum pressure and helium leak rate were monitored continuously. The cool down from room temperature to about 6 K was achieved within 24 days.

3.2 Warm up

The warm up of the cryostat was started on 17th of March 2016 and took 5 weeks with some interruption due to holiday period. The same criteria were applied for the warm up then for the cool down. The average warm

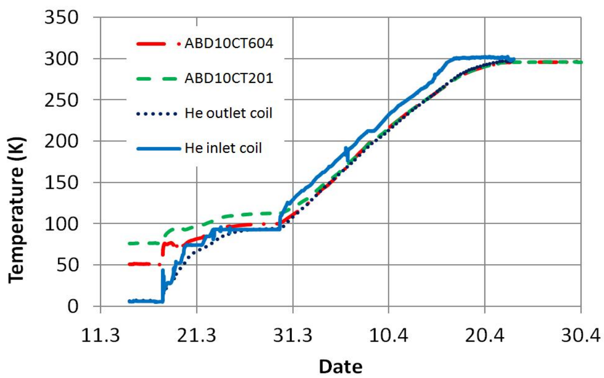

Fig. 5. Warm up of the W7-X cryostat. He in and outlet temperature of the coil casing cooling as well as shield temperatures are plotted.

up rate was 0.6 K/h. Thermal shield temperatures of PV, OV and helium outlet temperature of the shield cooling circuit are plotted against time (see Fig. 5). Additionally inlet and return temperatures of one NPC are added (AAB21). During Easter holidays the inlet temperature was set constant at about 96 K. The temperature difference between helium inlet and the shield panels decreased with increasing feed temperature.

4. Cooling during stationary operation

In the Standard Mode (SM) of the refrigerator the coils and the structures are cooled with helium at 3.9 K. Cold circulators pump helium through the housing and conductor cooling circuits. The thermal shield is cooled with helium at about 50 K at 13 bars. Over weekends the cryostat cooling is changed to the Short Standby Mode (SSM). This mode is characterized by return temperatures for the structure and conductor cooling between 6-10 K. The helium inlet temperature of the thermal shield varies from 40 to 50 K depending on the actual cooling conditions in the cryo plant. The cooling parameters are given in Table 1. During longer breaks the cryostat is warmed up to about 100 K in the Long Standby Mode (LSM).

Table 1. Cooling parameters conductor and housing cooling

	SM	SSM	LSM
Coil feed temperature	3.9 K	< 10 K	<100K
Flow coil housing	300 g/s	125 g/s	133 g/s
Flow coil conductor	200 g/s		
Inlet pressure housing	3.15 bar	1.8 bar	3.8 bar
Inlet pressure conductor	3.7 bar	2 bar	4.9 bar
Common outlet pressure	3.0 bar	1.8 bar	3.2 bar
Shield inlet temp.	40-50 K	40-50K	<100 K
Flow shield	134 g/s	134 g/s	87 g/s

4.1 Stationary thermal shield temperature

Fig. 6 shows the shield temperatures for the SSM with a helium feed temperature of 44 K. Table 2 summarizes the location of the sensors plotted in Fig. 6. The Helium inlet and outlet of the OV shield and the PV-outlet temperatures are the lowest in the diagram. Two out of five sensors of the PV-shield follow with temperatures at about 70 K. The other three PT100 sensors on the PV-shield show out of range as their temperature is below 65 K and are not plotted for the SSM. The OV-shield sensors differ by 9 K and show the highest values (77 K and 86 K).

Fig. 6 also shows the shield temperatures for the Long Standby Modus (LSM). In that mode the inlet temperature is set to 97 K. The temperature difference between outlet temperature and shield temperature is smaller than in the SSM (16 K instead of 28 K for HMX0), because of a better thermal conductivity with increasing temperature and a reduced heat load. The sequence of the temperatures in the plot is the same for the LSM as for the SSM except for the PV temperature CT102 which is higher than expected. All five PV-shield sensors are plotted. The outer vessel sensor 10CT202 has still the highest temperature.

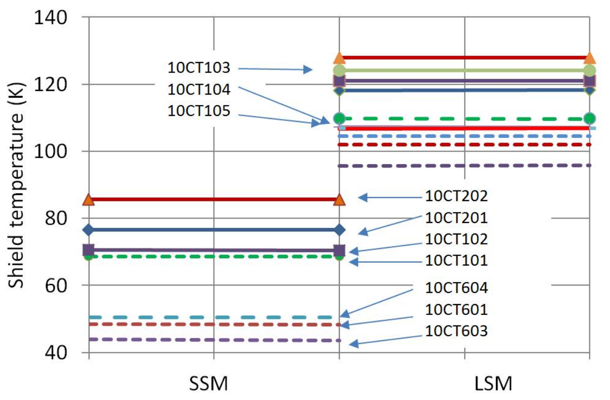

Fig. 6. OV and PV shield temperatures for SSM and LSM in HM10 together with cooling pipe temperatures.

Table 2. Overview of the shield sensor location.

	Outer vessel	Plasma vessel
At panel	10CT201- 202 11CT201	CT101-105
At cooling pipe	CT603 (inlet) CT601 (outlet)	CT601* (inlet) CT604 (outlet)

*OV helium outlet temperature is equal to PV inlet temperature.

The average temperature values for the OV-sensors for all 5 modules are given in Table 2. The sensors in HMX1 show temperatures about 20 K higher than in HMX0 because the position of these sensors is far away from the next cooling pipe and close to big port or dome shields and show hot spot values. The average OV temperature is calculated to 80 K neglecting the hot spot temperatures.

Table 3. Average OV-shield temperatures of all modules in the SSM

	HM X0	HM X1
CT201	79 K	101 K
CT202	81 K	105 K

The port shields have quite different sizes and show temperatures between 65 K and 112 K for the SSM in module 1. The average value matches the calculated average temperature of the OV-shield. In the LSM the minimum and the maximum temperature are 125 K and 143 K.

4.2 Heat load on the thermal shield

The thermal loads on the shield are plotted in Fig. 7 as a function of the shield inlet temperature. The heat load decreases roughly linear with increasing shield temperature indicating that thermal conduction is more relevant than radiation to the shield temperature load.

The average thermal load on the shield is 5.9 W/m² for a shield temperature of 50 K and matches the design value of 6 W/m^2. The sum of all shield panel surfaces was used for the calculation (A=948 m^2). 66 % of the thermal load is removed by the OV-shield cooling, 34 %

is removed by the PV-shield cooling. This ratio fits to the ratio of the cooled surface areas.

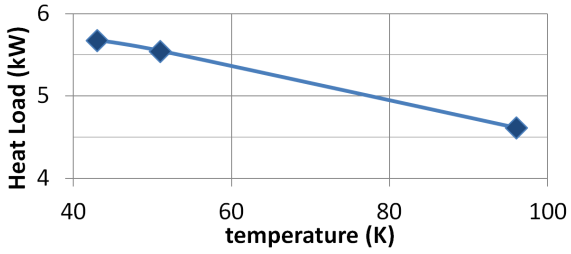

Fig. 7. Heat load at thermal shield for different shield inlet temperatures.

4.3 Temperatures of the coils

The 50 non planar coils have three temperature sensors on the casing of each coil and up to 6 sensors on the inlet and outlet pipes of the individual housing and conductor cooling. Fig. 8 shows the number of sensors that have temperatures in temperature interval of +/- 50 mK during SM. When operating in the SM the feed temperature is 3.9 K. The most frequent temperature is 4.1 K. Only a few sensors show temperatures above 4.7 K. The spread of values can be understood as the temperatures are measured on the pipe surfaces rather than in the fluid and hence are affected by small heat input from the surroundings. The average coil temperature of 4.2 K matches well with the helium return temperature of 4.18 K that is measured in the helium flow of the return line in a valve box.

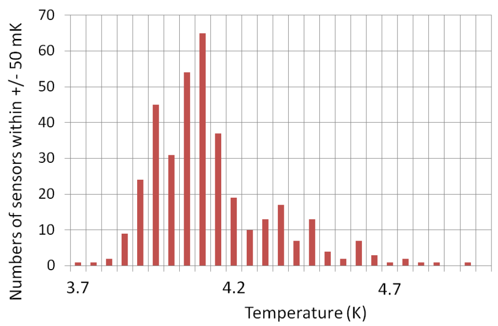

Fig. 8. Number of coil temperatures sensors within an temperature interval of +/- 50 mK for the SM.

In operation phase 1 the magnet system was operated with a current of 12.8 kA in the NPC and 5 kA in the PLC. In steady state condition the outlet temperatures of the conductor cooling are 50 mK higher than without current. The maximum allowed temperature was calculated to 5.16 K [4] taking into account a safety margin of 1 K against quench. The average outlet temperature with current in steady state condition is 0.96 K below the maximum allowed value. This gives enough safety margins for a safe operation.

4.4 Heat load on cold structure

The overall thermal load at the 4 K level is 572 W on the coils and 128 W on the Central Support Ring (CSR). These loads are much lower than the specified 1800 W for the refrigerator system. Dividing these numbers by the surface area of the components calculates to 0.67 W/m² and 0.85 W/m². Not the surface area but the projected surface area was considered as relevant to calculate the heat load for the CSR. The measured heat loads are smaller than the design value of 1.5 W/m² which included a safety factor of 1.5. The loads for the LSM are reported in table 3.

The heat load on the coils is compared with the calculated radiation of two concentric closely spaced spheres. This is justified as the areas of cold structure and shield are roughly the same. A common emissivity factor of $\varepsilon = 0.28$ is derived for shield and coil surface, from the heat loads for the LSM. Applying this emissivity to the SSM the calculated radiation load is 25 % lower than the measured value. This indicates that the heat load at 6 K is not only radiation but also heat conduction.

Table 4. Heat load on coils and CSR for different operation modes and different shield inlet temperatures.

Feed temp shield	Load on coils	Load on CSR
43 K (SSM)	426 W at 6 K	113 W at 4 K
96 K (LSM)	886 W at 98 K	201 W at 99 K

5. Summary

The cool down of the cryostat of Wendelstein 7-X was achieved in March 2015 within 4 weeks. The performance of the complex thermal insulation was confirmed. The heat loads on the thermal shield and on the cold structures were below the design values of the cryostat. The refrigerator capacity was sufficient to allow a safe operation of the superconducting magnet system. After this successfully experimental campaign the cryostat was warmed up to room temperature in March 2016. The next cool down will be performed after an upgrade of the divertor in 2017.

Acknowledgments

This work has been carried out within the framework of the EUROfusion Consortium and has received funding from the Euratom research and training program 2014-2018 under grant agreement No 633053. The views and opinions expressed herein do not necessarily reflect those of the European Commission.

References

[1] H.-S. Bosch et al., Experience with the Commissioning of the Superconducting Stellarator Wendelstein 7-X, Fus. Eng. Design 96-97 (2015) 22-27.

[2] Nagel, M. et al., Thermal and Mechanical Analysis of Wendelstein 7-X Thermal Shield; Proceedings of the Twenty-Third International Cryogenic Engineering Conference ICEC23 – ICMC2010, pp. 815-820.

[3] Nagel, M. et al., Cryogenic commissioning, cool down and first magnet operation of Wendelstein 7-X, Proceedings of the Twenty-Six International Cryogenic Engineering Conference ICEC26 – ICMC2016, accepted for publication.

[4] Baldzuhn, J. et al., Vacuum leak search on Wendelstein 7-X cryostat vessel, Vacuum 115 (2015) 89-100.